PAPER

Synthesis of novel triarylamine-based dendrimers with N⁴,N⁶-dibutyl-1,3,5-triazine-4,6-diamine probe for electron/energy transfers in H-bonded donor–acceptor–donor triads and as efficient Cu²⁺ sensors†

Muthaiah Shellaiah, Yesudoss Christu Rajan and Hong-Cheu Lin*

Two novel highly soluble triarylamine dendrimers **TPAD1** and **TPAD2** with N⁴,N⁶-dibutyl-1,3,5-triazine-4,6-diamine probe were synthesized *via* normal synthetic routes. Both dendrimers (**TPAD1** and **TPAD2**) form H-bonded donor–acceptor–donor (D–A–D) supramolecular triads **TPAD1-PBI-TPAD1** and **TPAD2-PBI-TPAD2** with 3,4,9,10-perylene tetra carboxylic diimide derivative (**PBI**). The presence of multiple H-bonds in the solution state was elucidated by ¹H NMR titrations and IR spectral studies. J-aggregations and electron/energy transfers provided by both dendrimers were verified by UV–Vis and photoluminescence (PL) titrations with **PBI** and the particle sizes of supramolecular triads were calculated by X-ray diffraction (XRD) analysis. Similarly, both dendrimers also showed sensitivities towards Cu²⁺ in comparison with 19 interfering metal ions, which were evidenced *via* UV–Vis and PL titraions in both single and dual metal systems. The maximum detection limit of Cu²⁺ ions was determined to be 20 ppm from PL titrations for both dendrimers, and the 1 : 2 stoichiometry of the complexes formed by both dendrimers (**TPAD1**-Cu²⁺ and **TPAD2**-Cu²⁺) were calculated by Job plots based on UV–Vis absorption titrations. More importantly, the binding mechanism of the 1,3,5-triazine-4,6-diamine probe of both dendrimers was well characterized by ¹H and ¹³C NMR titrations ([D₈] THF : D₂O = 2 : 1 in vol.) and supported by the fluorescence reversibility by adding metal ions and **PMDTA** sequentially.

Introduction

Due to their highly branched and symmetric structures, dendrimers have attracted great attention in the past few decades, which can be utilized for various applications including guest–host chemistry,[1] analytical chemistry,[2] optical data storage[3] and medical applications.[4] In addition, dendrimers have been designed as light-harvesting (LH) antennas in artificial photosynthesis because of their capability of directional excitation energy transfer (EET).[5] It is easy to imagine that dendrimers are also interesting scaffolds for photoinduced charge transfer from the core to the periphery, the number of units from the core to the periphery is at least doubled with each higher generation. At the same time, the supramolecular concept also attracted increasing attention in macromolecular science, as one can design new supramolecular architectures with interesting morphologies

derived from non-covalent interactions such as hydrogen bonds, van der Waals forces, π–π stackings, and dipole–dipole interactions.[6] Among these interactions, hydrogen bonds are more specific and highly directional in both solutions and surfaces, so they are widely used in the construction of three-dimensional supramolecular architectures in both chemical and biological systems.[7] Supramolecular controls over dye arrangements are important for both improving the performance of existing optoelectronic devices and creating new dye-based materials. Perylene bisimides (**PBI**) are widely applied as red dyes for industrial purposes owing to their favorable chemical, light and thermal stabilities.[8] In addition, several reports reveal that perylene bisimide forms H and J type aggregations with various triazine based donors.[9]

In a similar manner, chemosensors based on ion-induced fluorescence changes become increasingly popular due to their relative simplicity, sensitivity and selectivity.[10] Among the metals, Cu²⁺ is a significant metal pollutant due to its widespread use,[11] but it is also required as a cofactor in nearly 20 enzymes[12] and an essential micro-nutrient for all known life forms. In addition, most of the copper-selective sensors suffer from the interfering effect[13] of cations, such as Zn²⁺, Hg²⁺, Pb²⁺, Fe³⁺ and Ag⁺. Therefore, the development of a highly selective fluorescence probes[14] for copper ions in the presence of a variety of

Department of Materials Science and Engineering, National Chiao Tung University, Hsinchu 30049, Taiwan, ROC. E-mail: linhc@mail.nctu.edu. tw; Fax: +8863-5724727; Tel: +8863-5712121 ext.55305

8976 | *J. Mater. Chem.*, 2012, **22**, 8976–8987

This journal is © The Royal Society of Chemistry 2012

other metal ions has attracted great interest. Fluorescence sensors of Cu^{2+} ions are utilized to clarify the physiological roles[15] *in vivo* as well as to monitor their concentrations in the metal-contaminated sources[16] due to the high detection sensitivity and intrinsic operation simplicity of fluorescence sensors.

Since the sulfur and nitrogen donor atoms can be coordinated with transition-metal ions to form metal complexes, small size thiacrown ethers,[17] non-cyclic neutral ionophores,[18] calixarenes[19] and Schiff bases[20] have been used for ion carrier sensor applications. There are many polymeric materials[21] reported to be utilized as transition metal sensors, and also very recently nonconjugated dendritic molecules, such as poly(amidoamine) and poly(propylenimine) dendrimers, are developed as metal ion sensors.[22] However, to the best of our knowledge there is still only a few reports available in the literature for the sensor applications of conjugated dendritic molecules[23] *via* energy transfers from fluorescence sensors (to be quenched) to metal ions. The energy transfers in fluorescent dendrimers prevailed in nano-structural materials.[24] Triarylamine dendrimers have important roles in the applications of organic LEDs[25] and organic solar cells,[26] because of their excellent thermal and electrochemical stabilities, electron donating and charge-transporting abilities, and transparent properties, as well as three-dimensional propeller structures.[27] The triazine[28] core derivatives also enhance energy transfer processes in various supramolecular architectures, and the greater affinities of the triazine units demonstrate that they may act as useful spacers as well as selective receptors for sensors and supramolecules.

Literature reports[29] of triarylamine derivatives containing conjugated structures also proved to be excellent fluorescence sources, and hence provide enough flexibility to construct novel fluorescent triarylamine dendritic moieties with a triazine core for energy transfer in supramolecules as well as for metal sensor applications.

Herein, we report the synthesis of novel triarylamine-based dendrimers **TPAD1** and **TPAD2** with a N^4,N^6-dibutyl-1,3,5-triazine-4,6-diamine probe[30] for efficient electron/energy transfers in perylene bisimide (**PBI**)-based donor–acceptor–donor H-bonded nano-sized J-aggregation of supramolecular triads. For the first time, their sensing capabilities towards various metal ions were investigated by UV–Vis and fluorescence spectroscopies. Both dendrimers **TPAD1** and **TPAD2** show high selectivity towards Cu^{2+} ions *via* the turn-off fluorescence mechanism (Fig. 1) in the presence of other transition and non-transition metal ions in semi-aqueous media (THF : H_2O = 2 : 1 in vol.) at pH = 7.0 (at 25 °C).

Results and discussion

Synthesis

The 3,4,9,10-perylene tetracarboxylic diimide derivative (**PBI**) was synthesized according to the previous literature[31] with required purity and the synthetic procedures of dendrimers **TPAD1** and **TPAD2** were shown in Schemes 1–3, where the introduction of hexyloxy groups in compounds **2** and **4** provides good solubilities to the dendritic molecules. Compounds **2** and **4** reacted in the presence of L-proline and CuI as catalysts to afford compound **5**. Compounds **7** and **8** were synthesized according to

the literature,[32,33] and compounds **9** and **11** were obtained by reacting compound **8** with compounds **5** and **10**, respectively, to reflux in toluene for 72 h in the presence of catalytic amounts of tri-*tert*-butylphosphine, palladium acetate, and cesium carbonate. Dendrons **10** and **12** were obtained from compounds **9** and **11**, respectively, by Claisen's base treatments.[33] Then, compounds **10** and **12** were reacted with cyanuric chloride **13** in THF at 0 °C in the presence of catalytic amounts of diisopropylethylamine (**DIPEA**). After this reaction, the crude product was refluxed with butylamine, using sodium bicarbonate as a catalyst and dioxane as a solvent to provide the final dendrimers (**TPAD1** and **TPAD2**) with high purities.

(a) Formation of (D–A–D) supramolecular triads

IR spectra. As shown in Fig. 2, the attenuated total reflection Fourier transform infrared (ATR-FTIR) spectra of **TPAD1**, **TPAD2** and **PBI** in CH_2Cl_2 showed free NH stretching bands at 3428, 3410 and 3170 cm^{-1}, respectively. The NH stretching bands of supramolecular triads **TPAD1-PBI-TPAD1** and **TPAD2-PBI-TPAD2** (2 : 1 stoichiometry) in CH_2Cl_2 were observed at 3317 and 3318 cm^{-1}, respectively, which confirmed the formation of multiple hydrogen bonds between the H-bonded donors and acceptors.[34]

^1H NMR titrations. To reconfirm the presence of multiple hydrogen bonds in triad complexes, we performed the ^1H NMR titrations as shown in Fig. S21 and S22 (ESI),† in which the **PBI** concentration was kept constant at 10 mM and the concentrations of dendrimers **TPAD1** and **TPAD2** increased up to 2.5 equivalents with an equal span of 0.5 equivalent. When increasing the cocentrations from 0 to 2.5 equivalents, the NH protons of **PBI** showed downfield shifts in both supramolecular triads from 8.44 to 9.66 ppm and from 8.44 to 9.75 ppm for **TPAD1-PBI-TPAD1** and **TPAD2-PBI-TPAD2**, respectively. The down-field shifts of **PBI**-NH protons were also evidence for the formation of multiple hydrogen bonds in the supramolecular complexes as per the literatures.[35] Fig. 3 illustrated the changes in the chemical shifts of NH (**PBI**) with respect to the concentrations of both dendrimers (**TPAD1** and **TPAD2**). During these titrations, some up-field shifts in triazine NH protons of **TPAD1** and **TPAD2** were found, but the triazine NH protons were not distinguishable because of the greater crowding in their alkyl chain regions. The presence of multiple hydrogen bonds and energy transfers as well as aggregation types were well established by UV/PL titrations in low polarity solvents, such as methylcyclohexane (MCH), which is shown in the next section.

UV–Vis and PL titrations. UV–Vis and PL titration experiments in methylcyclohexane (MCH) were performed to study the interactions of both dendrimers (**TPAD1** and **TPAD2**) with **PBI**. Upon adding aliquots of **TPAD1** to **PBI**, a bathochromic shift (Fig. 4a) from 562 to 567 nm was observed in the perylene absorption maximum of the S_0–S_1 electronic transition for **TPAD1-PBI-TPAD1**. However, this shift was larger in **TPAD2-PBI-TPAD2**, *i.e.*, from 562 to 570 nm (Fig. 4b). Similar to the titrations of absorption spectra, the PL titrations of fluorescence spectra in both supramolecular triads (Fig. 4c and 4d) showed bathochromic shifts in **TPAD1-PBI-TPAD1** (from 591 nm to 596 nm) and **TPAD2-PBI-TPAD2** (from 591 nm to 599 nm).
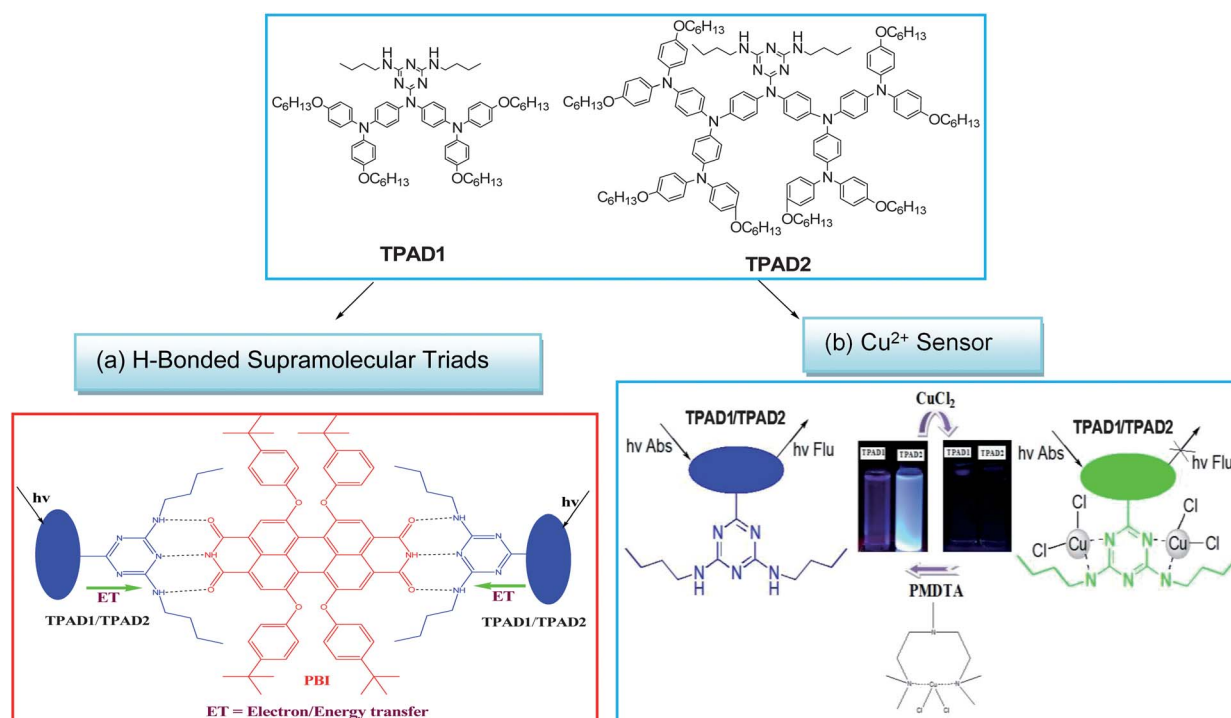
Fig. 1 Structures of triarylamine-based dendrimers (**TPAD1** and **TPAD2**): (a) schematic representation of electron/energy transfer in supramolecular triads of **PBI** with **TPAD1** and **TPAD2**; (b) schematic representation of Cu²⁺ sensor responses provided by **TPAD1** and **TPAD2**.

Both results of UV–Vis and PL titrations verified that the perylenes pack tightly in a J-type aggregation in supramolecular triads. Ordinary J-aggregated dyes showed intense fluorescence during the titration of supramolecular formation. Here the PL titrations of the perylene was also enhanced ($\lambda_{ex} = 575$ nm, $\lambda_{em} = 591$ nm) by adding both dendrimers (**TPAD1** and **TPAD2**). This consequence was rationalized by an electron/energy-transfer process from the dendrimers (**TPAD1** and **TPAD2**) to the perylene chromophore (**PBI**), and the optimal enhanced fluorescence was obtained as **PBI** was fully H-bonded to **TPAD1** (or **TPAD2**) at a ratio of 1 : 2.

The electron/energy transfers as well as the presence of J-aggregation in both supramolecular triads were well demonstrated by UV–Vis and PL titration experiments. During UV–Vis titrations, dendrimers **TPAD1** and **TPAD2** showed isosbestic points at 368 and 398 nm, respectively, which arose from the

energy/electron transfers by multiple H-bonded complexes in MCH solutions. The titration analysis of both supramolecular triads (**TPAD1-PBI-TPAD1** and **TPAD2-PBI-TPAD2**) in Fig. 4 showed the formation of 2 : 1 H-bonded triads as reported previously.[36] Since the formation of multiple H-bonds in the supramolecular triads were well supported by UV–Vis, PL and ¹H NMR titrations along with ATR-FTIR spectra, further investigations of particle size of both supramolecular triads were carried out *via* X-ray diffraction (XRD) analysis of powder samples on glass substrates.

X-ray diffraction (XRD) analysis. As evidenced in Fig. 5, the powder XRD patterns of **TPAD1**, **TPAD2**, **PBI** and supramolecular triads (see the experimental procedure in the ESI† for the preparation of triads **TPAD1-PBI-TPAD1** and **TPAD2-PBI-TPAD2**) were taken on glass substrates at room temperature.
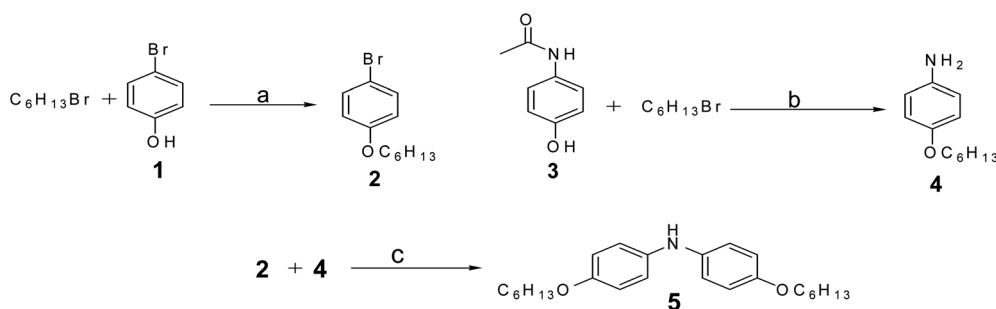

Scheme 1 (a) Me₂CO/K₂CO₃, 90%; (b) (i) Me₂CO/K₂CO₃, (ii) C₂H₅OH: HCl (6 : 4), 100 °C, 92%; (c) DMSO/K₂CO₃, CuI, ʟ-proline, 90 °C, 24–30 h, 84%.
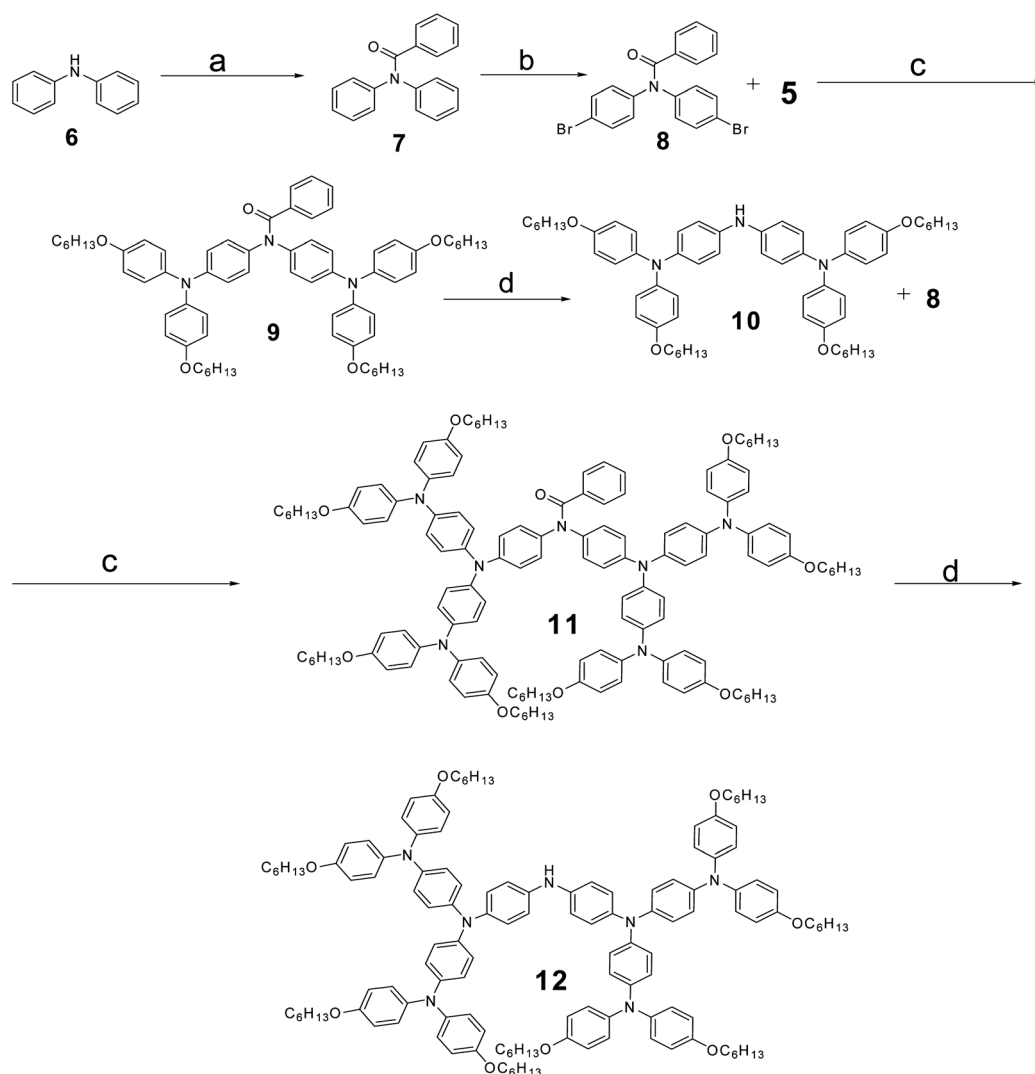
Scheme 2 (a) Benzoyl chloride, pyridine, 0 °C, 92%; (b) Br$_2$, CH$_2$Cl$_2$, 40 °C, 90%; (c) Pd(OAc)$_2$, P(t-Bu)$_3$, Cs$_2$CO$_3$, toluene, 110 °C, 72h, 72%/64% (**9/11**); (d) Claisen's base, THF–H$_2$O, reflux, 12 h, 99% (**10** and **12**).

The donors (**TPAD1** and **TPAD2**) and acceptor (**PBI**) showed strong Bragg diffractions, but significantly decreased in intensities with broader peaks after the formation of multiple H-bonds between dendrimers and **PBI**. The XRD peak values of supramolecular triads were 17.60° and 25.69° for **TPAD1-PBI-TPAD1** and 15.58° and 25.09° for **TPAD2-PBI-TPAD2**. The particle sizes of supramolecular triads **TPAD1-PBI-TPAD1** and **TPAD2-PBI-TPAD2** were calculated using the Scherrer formula.[37] Particle size (D) = 0.9λ/βcosθ, where λ, β and θ represent the X-ray wavelength (1.5406 Å), FWHM (radian) value of diffraction

peak and Bragg diffraction angle, respectively, at room temperature. The diffraction angles (θ), FWHM values and their calculated lattice d spacings of supramolecular triads (**TPAD1-PBI-TPAD1** and **TPAD2-PBI-TPAD2**) are revealed in Table 1. The average particle sizes of **TPAD1-PBI-TPAD1** and **TPAD2-PBI-TPAD2** are 9.72 and 10.45 Å, respectively. Attempts to observe the self-assemblies of microscopic images and to measure the photocurrent efficiencies of thin film transistors for both supramolecular triads were in vain due to their poor film qualities.
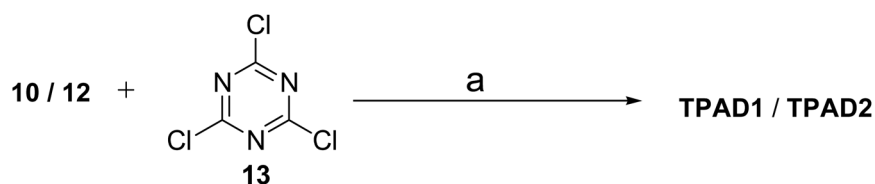
Scheme 3 (a) (i) Diisopropyl ethylamine, THF, 0 °C, (ii) BuNH$_2$, NaHCO$_3$, dioxane, 100 °C, 85%/78% (**TPAD1/TPAD2**).

This journal is © The Royal Society of Chemistry 2012

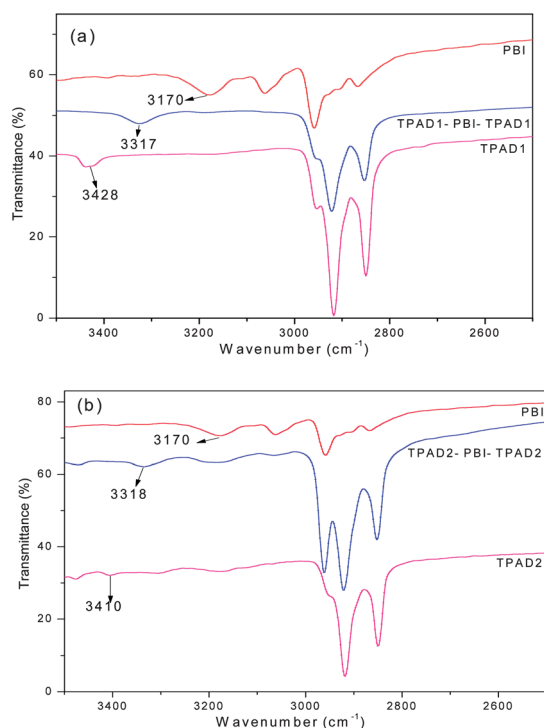*J. Mater. Chem.*, 2012, **22**, 8976–8987 | **8979**

Fig. 2 ATR-FTIR spectra of (D–A–D) supramolecular triads in CH_2Cl_2 with 2 : 1 ratio of (a) **TPAD1** and **PBI**; (b) **TPAD2** and **PBI**.
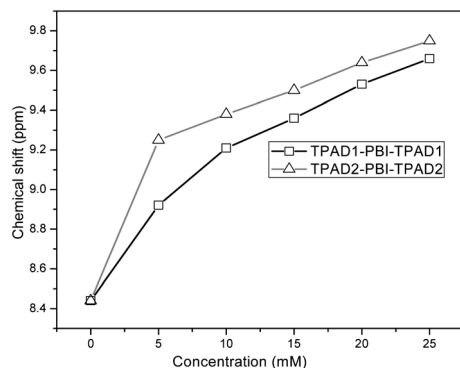

Fig. 3 ^{1}H NMR shifts of N–H protons (in **PBI**) for supramolecular triads formed by complexation of **PBI** with **TPAD1** and **TPAD2**, respectively, where the **PBI** concentration was fixed at 10 mM.

(b) Dendrimers as Cu²⁺ sensors

Optical properties. Both dendrimers **TPAD1** and **TPAD2** exhibited absorption maxima (see Fig. S27 in ESI†) at 308 and 314 nm, respectively. The little red-shifted and broadening absorption peak of **TPAD2** were due to the extended conjugation in the higher generation of the dendritic structure in contrast to **TPAD1**. As shown in Fig. S28 of the ESI,† both dendrimers **TPAD1** and **TPAD2** provided PL emission maxima at 398 and 427 nm, respectively, and their photophysical properties are shown in Table 2.

Both dendrimers showed great solubilities in THF : water = 2 : 1, but the water content was increased further by adding metal ion solutions (in water) to the dendrimer solutions (in THF : water = 2 : 1). Therefore, we chose the solvent condition

as THF : water = 4 : 1 (vol.) for the sensor titrations of both dendrimers (**TPAD1** and **TPAD2**), and the final solvent composition was maintained as THF : water = 2 : 1 (vol.) after titrations for both dendrimers. The quantum yields (Table 2) of both dendrimers also showed that the above solvent system was highly suitable for the sensor system. Hence, we performed UV–Vis/PL titrations of both dendrimers in THF : H_2O (4 : 1 in vol.) and ^{1}H, ^{13}C NMR titrations in [D_8] THF by adding metal ions in pure H_2O and D_2O, respectively.

Fluorescence titrations on metal ions. To prove the specific selectivity of this dendritic sensory system, almost 20 metal ions from their respective water soluble sources were chosen and the titrations performed as shown in Fig. 6. Upon addition of 2 equiv. of aqueous solutions (40 μM in H_2O) with different metal ions to the solutions (20 μM in THF : H_2O = 4 : 1 in vol.) of dendrimers **TPAD1** and **TPAD2**, emission maxima at 398 and 427 nm (with an excitation at 308 and 314 nm) were seen, respectively. It shows that Cu^{2+} has a relatively higher fluorescence quenching capability among the coexisting transition (d-block) metal ions (such as Cu^+, Ag^+, Co^{2+}, Fe^{2+}, Mn^{2+}, Zn^{2+}, Ni^{2+}, Hg^{2+}, Ag^{2+} and Fe^{3+}), and non transition (s and p blocks) metal ions (such as Li^+, Na^+, K^+, Cs^+, Ba^{2+}, Ca^{2+}, Pb^{2+}, Mg^{2+} and Al^{3+}). The above observations also support that the sensitivities of both dendrimers to Cu^{2+} ions were much better even in the presence of interfering metal ions, such as Fe^{3+}, Zn^{2+}, Hg^{2+}, Pb^{2+} and Ag^+. However, **TPAD1** has a slightly lower selectivity towards Cu^{2+} ions than **TPAD2**, which was clearly revealed by the lower fluorescence intensity of **TPAD1** with a shorter dendritic conjugation length.

The better sensing capabilities of **TPAD1** and **TPAD2** toward Cu^{2+} ions were also verified in Fig. 7, where dendrimer **TPAD2** shows three times higher sensitivity than **TPAD1**, because of its higher generation structure and hence greater energy transfer[38] in contrast to **TPAD1**. This can be explained by the fact that as the dendritic generation increases, the π–π conjugation increases to improve the electron or energy transfer. Selectivities of both dendrimers (**TPAD1** and **TPAD2**) towards Cu^{2+} ions possibly arise from the ligand to metal electron/energy transfer[39] but it might be essential to estimate the concentration limits of copper ion detections by these dendritic molecules, which can be performed by the UV–Vis/PL titrations. Moreover, the binding site of the present sensor dendritic system with Cu^{2+} ions was confirmed through the evidence of NMR spectral titrations, and the reversibility of binding behaviour can be detected by the UV–Vis and fluorescence titrations. Consequentially, the stoichiometry of the metal complexes can be proven from the Job plots of UV–Vis absorbance titrations for dendrimers **TPAD1** and **TPAD2**.

Fluorescence titrations of Cu^{2+} ions. By increasing the concentrations of Cu^{2+} (0–24 μM with an equal span of 2 μM in H_2O), the sensitivities of **TPAD1** and **TPAD2** towards Cu^{2+} ions were clearly observed in Fig. 8. The fluorescence spectra of dendrimers **TPAD1** and **TPAD2** were quenched rapidly, and Fig. 8c and 8d clearly illustrate that their quenching effects were saturated at the concentration of 20 μM for Cu^{2+} ions. The saturation points identified here represent the complete quenching of both dendrimers and hence the maximum detection

8980 | *J. Mater. Chem.*, 2012, **22**, 8976–8987

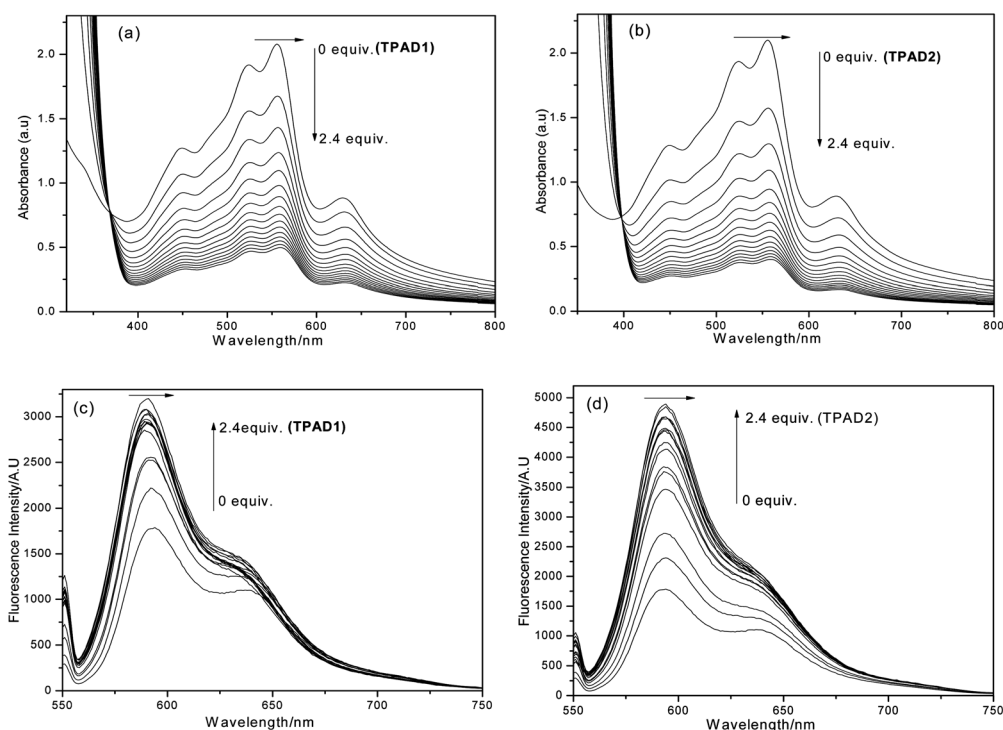This journal is © The Royal Society of Chemistry 2012

Fig. 4 UV–Vis (a), (b), and PL (c), (d) titrations of **TPAD1-PBI-TPAD1**, and **TPAD2-PBI-TPAD2** in methyl cyclohexane (MCH) (the concentration of **PBI** was kept constant as 1 equivalent at 1×10^{-5} mol L^{-1}) upon the addition of **TPAD1** and **TPAD2** at different concentrations (0–2.4 equivalents with equal span of 0.2 equivalents).
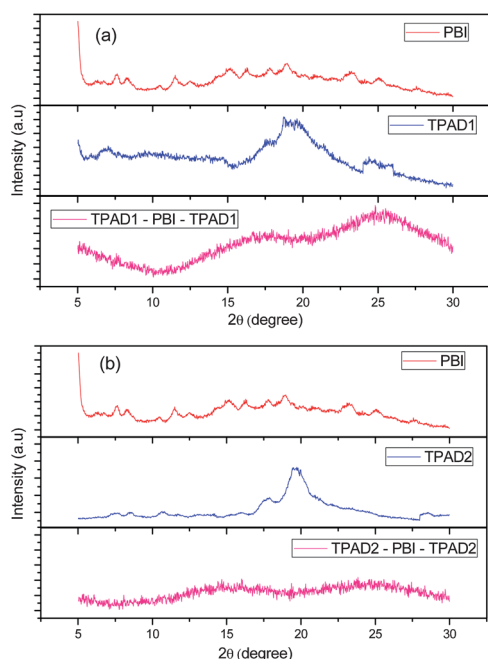

Fig. 5 XRD patterns of compounds. (a) **PBI**, **TPAD1** and **TPAD1-PBI-TPAD**; (b) **PBI**, **TPAD2** and **TPAD2-PBI-TPAD2** on glass substrates at room temperature.

Table 1 Diffraction angles (2θ), FWHM values, lattice spacings and particle sizes of **TPAD1-PBI-TPAD1** and **TPAD2-PBI-TPAD2**

H-bonded complex	TPAD1-PBI-TPAD1		TPAD2-PBI-TPAD2	
	$2\theta_1$	$2\theta_2$	$2\theta_1$	$2\theta_2$
$2\theta/°$	17.60	25.69	15.58	25.09
FWHM/°	7.60	9.09	7.20	8.32
FWHM/radians	0.133	0.159	0.126	0.145
d spacing/Å	6.82	3.85	7.62	4.35
Particle size/Å	10.57	8.87	11.13	9.78
Average particle size/Å	9.72		10.45	

Table 2 Photophysical properties of **TPAD1** and **TPAD2**

Compound	λ_{max}/nm	λ_{em}/nm	Φ
TPAD1	308	398	0.273[a]
			0.231[b]
			0.253[c]
TPAD2	314	427	0.481[a]
			0.425[b]
			0.469[c]

[a] THF. [b] THF : water (2 : 1). [c] THF : water (4 : 1) and 2-aminopyridine in 0.1 M H_2SO_4 ($\Phi = 0.6$) was used as a standard reference.

limit of Cu^{2+} ions was justified as 20 ppm, as reported in the literature.[40] The above statement was further confirmed *via* Cu^{2+} ion titrations in the presence of different background metal ions as illustrated in Fig. 9. In this case, two equal amounts of

aqueous solutions of Cu^{2+} and other metal ions (20 μM + 20 μM) were combined, as well as the mixed aqueous solution of Cu^{2+} and all other metal ions (20 μM + 20 μM). Therefore, the sensitivities of **TPAD1** and **TPAD2** towards Cu^{2+} ions can be well
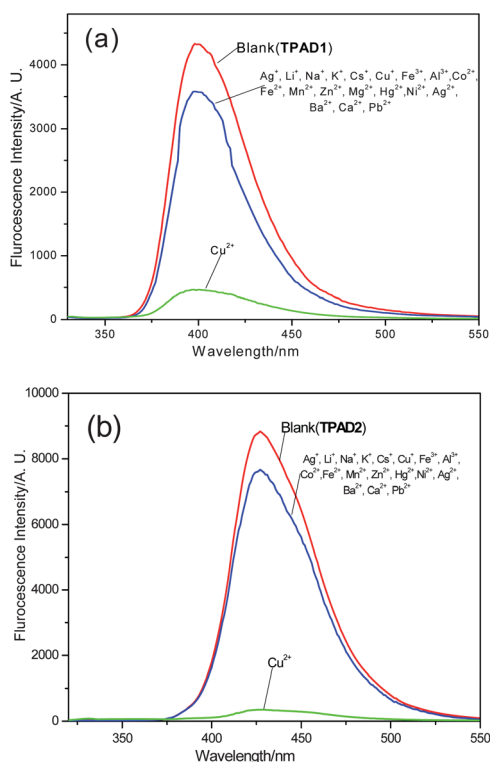
Fig. 6 Fluorescence spectra of (a) **TPAD1** (20 μM in THF : H$_2$O = 4 : 1 in vol.) and (b) **TPAD2** (20 μM in THF : H$_2$O = 4 : 1 in vol.) in the absence and presence of different metal ions (40 μM in H$_2$O) with excitations at 308 and 314 nm, respectively. The final solvent composition after titrations was THF : H$_2$O = 2 : 1 in vol. (due to similar fluorescence intensities for all metal ions other than Cu^{2+}, the average values were taken for simplicity).

demonstrated, which explains the sensing abilities of **TPAD1** and **TPAD2** in the presence of different metal ion backgrounds. In both cases of **TPAD1** and **TPAD2**, the sensitivities were little affected by the presence of the other metal ions, but **TPAD2** shows a greater sensitivity than **TPAD1** because of the higher generation and stability in **TPAD2**. This result was also well supported by Stern–Volmer constants (K_{SV}) shown in Table 3.

Characterization of binding site.[41] *and reversibility.*[42] The binding site of the sensor system can be evaluated by the NMR titrations of both dendrimer solutions, in which **TPAD1** and **TPAD2** were dissolved in [D$_8$] THF (1 × 10^{-3} M), with Cu^{2+} ion solutions in D$_2$O (2 × 10^{-2} M). During the addition of 2 equivalents of Cu^{2+} ions to 1 equivalent of dendritic compounds (**TPAD1/TPAD2**), the spectra in Fig. 10 show complete disappearance of NH proton peak at 2.51 and 2.44 ppm, for TPAD1 and TPAD2, respectively which may arise from the dehydration induced by Cu^{2+} ions. However, the broadening of the NMR spectra also occurs due to the presence of Cu^{2+} ions in the complex systems. To confirm the above statement, we also performed the titrations without Cu^{2+} ions (Fig. S25 and S26 in the ESI†) and it was confirmed that the dehydration as well as the broadening of ^{1}H NMR spectra arose only from the presence of Cu^{2+} ions. Due to the complex formation, small down-field shifts were observed for NH protons in both cases. In addition, as shown in Fig. 10, the nearby CH$_2$ protons were also up-field
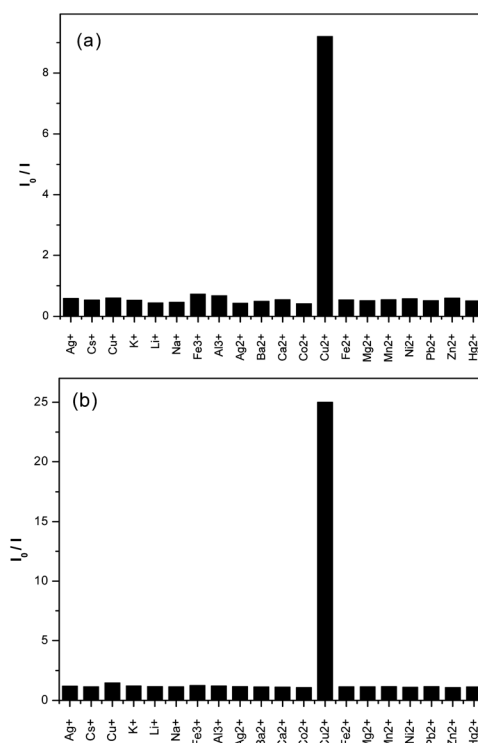

Fig. 7 Fluorescence responses of (a) **TPAD1** (20 μM in THF : H$_2$O = 2 : 1 in vol.) and (b) **TPAD2** (20 μM in THF : H$_2$O = 4 : 1 in vol.) in the absence and presence of different metal ions (40 μM in H$_2$O) with excitations at 308 and 314 nm, respectively. The final solvent composition after titrations was THF : H$_2$O = 2 : 1 in vol.

shifted from 3.28 to 3.17 ppm and from 3.27 to 3.16 ppm for **TPAD1** and **TPAD2**, respectively. This ^{1}H NMR spectral evidence also clearly signifies that the diamine probe attached to the triazine core is involved in the detection of copper ions, and justifies that triazine with diamine probe may act as a binding site in both **TPAD1**-Cu^{2+} and **TPAD2**-Cu^{2+} complexes. The ^{1}H NMR titration results of **TPAD1** and **TPAD2** supports the working principle of dendritic sensors *via* dehydration in the semi-aqueous medium THF : H$_2$O (2 : 1 in vol.).

The ^{1}H NMR titrations of both dendrimers only proved the involvement of the diamine probe attached to the triazine core in the sensing mechanism but not of just the triazine core. Therefore, we tried to evaluate the participation of the triazine core in the sensing mechanism *via* ^{13}C NMR titrations (Fig. S23 and S24 in the ESI†) of **TPAD1** and **TPAD2** in [D$_8$] THF (1 × 10^{-3} M) with Cu^{2+} ions in D$_2$O (2 × 10^{-2} M). The obtained results in ^{13}C NMR titrations proved the involvement of the triazine core in the sensing mechanism, and **TPAD1** showed two new peaks (green circles) at 176.27 and 155.13 ppm corresponding to the diminished peaks (red circles) at 168.41 and 147.66 ppm, respectively. Similarly, **TPAD2** also exhibited two new peaks (green circles) at 176.27 and 154.56 ppm, corresponding to the diminished peaks (red circles) at 168.45 and 147.81 ppm, respectively. Upon the addition of 2 equivalents of Cu^{2+} ions in D$_2$O solutions to 1 equivalent of both dendrimers (**TPAD1** and **TPAD2**) in THF [D$_8$] solutions, totally different ^{13}C NMR spectra appeared in comparison with the original ones.
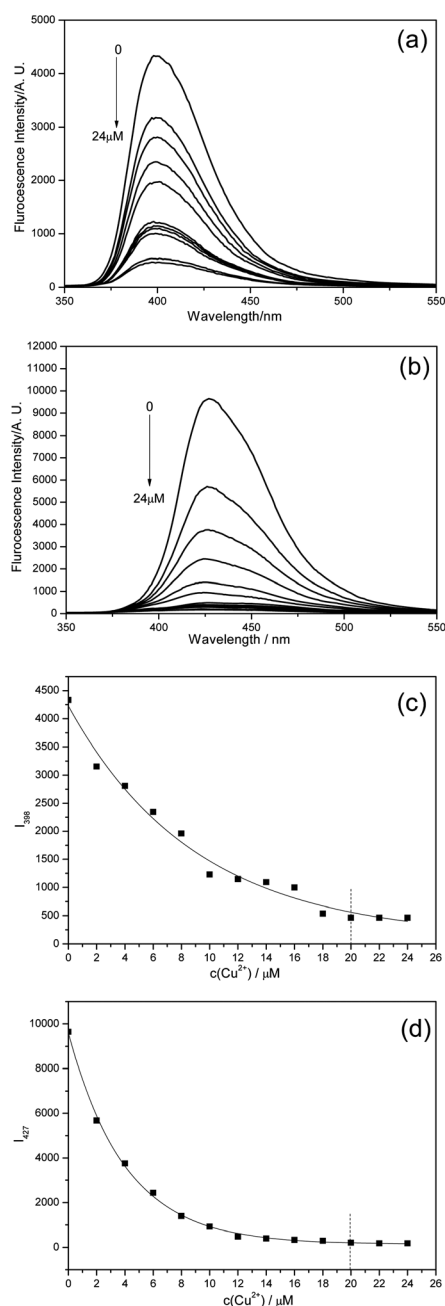
Fig. 8 Fluorescence spectra of (a) **TPAD1** (20 μM in THF : H₂O = 4 : 1 in vol.) and (b) **TPAD2** (20 μM in THF : H₂O = 4 : 1 in vol.) upon increasing concentrations of Cu^{2+} (0–24 μM with an equal span of 2 μM in H₂O), where the excitation wavelengths were 308 and 314 nm, respectively. (c) and (d) fluorescence maximum intensities of **TPAD1** and **TPAD2** as a function of Cu^{2+} concentrations.
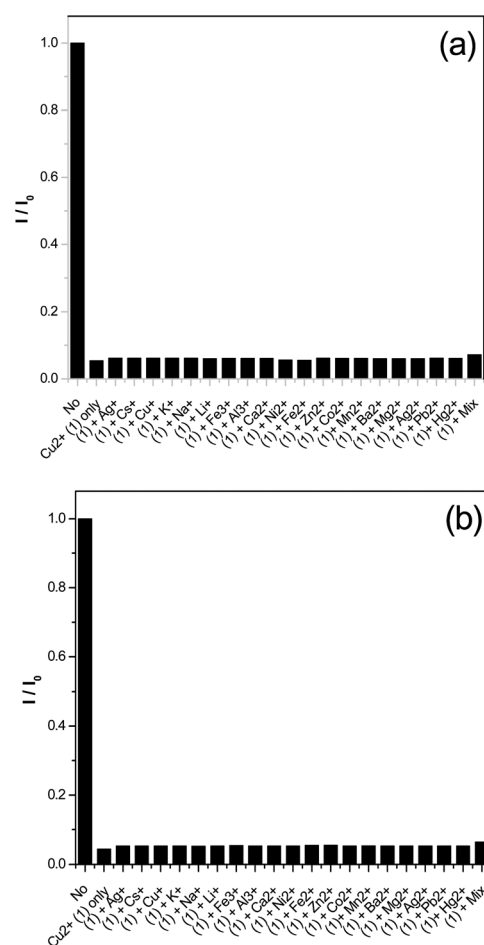

Fig. 9 Fluorescence responses of (a) **TPAD1** (20 μM in THF : H₂O = 4 : 1 in vol.) and (b) **TPAD2** (20 μM THF : H₂O = 4 : 1 in vol.) in the absence and presence of different metal ions (40 μM in H₂O) with excitations at 308 and 314 nm, respectively. The final solvent composition after titrations was THF : H₂O = 2 : 1 in vol.

The possible approaches of Cu^{2+} ions towards the triazine binding site are shown in Fig. 11. However, according to the stability concern,[43] symmetrical approaches were preferred to unsymmetrical ones and the results of ^{13}C NMR titrations also verified the above statement. Hence, we propose a similar approach mechanism of Cu^{2+} ions towards the triazine core as shown in Fig. 1 (schematic representation of Cu^{2+} sensor response) and these results are also well supported by the 1 : 2 stoichiometry of the Cu^{2+} complexes obtained in Fig. 13c and

13d. In general, binding sites are confirmed through the reversibility of the system; therefore, the reversible nature of the sensor complexes with Cu^{2+} ions was further investigated through UV–Vis and fluorescence spectroscopies by adding pentamethyl ethylene triamine[44] (**PMDTA**) dissolved in THF (1×10^{-5} M). In order to maintain the final solvent composition of THF : H₂O = 2 : 1 (vol.), we also used the same equivalent of **PMDTA** as Cu^{2+} ions. Upon the addition of **PMDTA** to the Cu^{2+} complexes (**TPAD1**-Cu^{2+} and **TPAD2**-Cu^{2+}) the reversible nature of the both sensor systems are evidenced in Fig. S29 (see ESI†). Both UV–Vis absorbance and fluorescence spectra of **TPAD1** (Fig. S29a and S29c in the ESI†) and **TPAD2** (Fig. S29b and S29d in the ESI†) clearly indicate the sensor reversibility. This evidence provides enough confidence for reusing the sensor probes, and hence further investigations were carried out to establish the number of reversible cycles. Both dendrimers (**TPAD1** and **TPAD2**) provided the sensor reversibilities of *ca.* 90% up to 10 cycles (Fig. 12c and 12 d), so it was evident that both dendrimers could be reused several times. In Fig. 12a and 12b, photographs of visualized reversibilities in **TPAD1** and **TPAD2** by the naked eye as well as by commercial

Table 3 Stern–Volmer constants (K_{SV}) of different metal ions

Metal ions[a]	**TPAD1** (λ_{abs} = 308 nm; λ_{em} = 398 nm) K_{SV} (M^{-1})[b]	**TPAD2** (λ_{abs} = 314 nm; λ_{em} = 427 nm) K_{SV} (M^{-1})[b]
Ag^+	2.05×10^3	9.93×10^3
Cs^+	2.30×10^3	7.61×10^3
Cu^+	1.95×10^3	2.35×10^4
K^+	2.33×10^3	1.08×10^4
Li^+	2.79×10^3	7.89×10^3
Na^+	2.70×10^3	7.14×10^3
Fe^{3+}	1.35×10^3	1.28×10^4
Al^{3+}	1.60×10^3	1.03×10^4
Ag^{2+}	2.86×10^3	7.92×10^3
Ba^{2+}	2.54×10^3	7.12×10^3
Ca^{2+}	2.26×10^3	5.79×10^3
Co^{2+}	2.91×10^3	4.16×10^3
Cu^{2+}	4.10×10^5	1.20×10^6
Fe^{2+}	2.28×10^3	7.54×10^3
Mg^{2+}	2.41×10^3	7.14×10^3
Mn^{2+}	2.26×10^3	8.43×10^3
Ni^{2+}	2.01×10^3	5.54×10^3
Pb^{2+}	2.43×10^3	8.40×10^3
Zn^{2+}	1.98×10^3	3.96×10^3
Hg^{2+}	2.44×10^3	6.44×10^3

[a] All metal ion concentrations were taken as 20 μM in H_2O from their respective aqueous solutions and dendrimer (**TPAD1** or **TPAD2**) concentrations were kept constant at 20 μM in THF : H_2O = 4 : 1 in vol. [b] K_{SV} = [(I_0/I) − 1]/[Q]; [Q] = quencher concentration (20 μM for all metal ions).

UV lamps (λ = 365 nm) were demonstrated. The formation of pale green/blue color during the addition of Cu^{2+} ions may be due to the formation of **TPAD1**-Cu^{2+} and **TPAD2**-Cu^{2+} complexes.

Stoichiometry calculation.[45] *by Job plots* UV–Vis absorption spectral titration results were shown in Fig. 13a and 13b. Both concentrations of dendrimers (**TPAD1** and **TPAD2**) were kept constant (20 μM in THF : H_2O = 4 : 1 vol/vol), and during the addition of Cu^{2+} ions in H_2O the formation of Cu^{2+} complexes with dendrimers (**TPAD1** and **TPAD2**) were confirmed by the appearance of new peaks at 405 and 439 nm, respectively. Upon addition of Cu^{2+} ions from 0 to 60 μM, the initial absorbance maxima of both dendrimers at 308 and 314 nm were found to have decreased and the peaks at 405 and 439 nm increases slowly. However, the peaks at 405 and 439 nm start quenching slowly upon addition of 30 μM and 38 μM aqueous solutions of Cu^{2+} ions to dendritic solutions of **TPAD1** and **TPAD2** (20 μM in THF : H_2O = 4 : 1 vol/vol), respectively. More interestingly, the appearances of two isosbestic points for **TPAD1** (281 and 343 nm) and **TPAD2** (281 and 376 nm) indicate the presence of simple equilibrium in the Cu^{2+} complexes. Further investigations of Job plots occurred at 405 nm (**TPAD1**) and 439 nm (**TPAD2**) against the mole fractions (X_M = [Cu^{2+}]/[Cu^{2+}] + [**TPAD1**] or [**TPAD2**]) of **TPAD1**-Cu^{2+} and **TPAD2**-Cu^{2+} complexes. Fig. 13c and 13d represent the Job plots of **TPAD1** and **TPAD2**, respectively, which indicate the formation of 1 : 2 stoichiometric complexes by both dendrimers. Two plots of (A_0–A_1) versus X_M show that (A_0–A_1) values go through a maximum at a molar fraction of *ca.* 0.59 (**TPAD1**) and 0.65 (**TPAD2**) in Fig. 13c and 13d, respectively, indicating a 1 : 2 stoichiometric complex formation. This was also supported by ^1H and ^{13}C NMR spectral titrations of **TPAD1** and **TPAD2** upon addition of 2 equivalents of Cu^{2+} ions (in D_2O) to 1 equivalent solution of both dendrimers (in [D_8] THF). The complete disappearance of

NH protons in ^1H NMR titrations (Fig. 10) and the appearance of two new peaks in conjunction with the complete disappearance of corresponding peaks in ^{13}C NMR titrations (Figs. S23 and S24†) upon the addition of 2 equivalents of Cu^{2+} ions in D_2O also support the 1 : 2 stoichiometry. According to these results, the formation of dimeric complexes by Cu^{2+} ions was further confirmed, and hence the probable 1 : 2 stoichiometric complexes for both dendrimers **TPAD1** and **TPAD2** were proposed as shown in Fig. 11. Table 3 shows Stern–Volmer quenching constants (K_{SV})[46] of different metal ions, calculated from K_{SV} = [(I_0/I) − 1]/[Q], where [Q] is the quencher concentration. The detection limit of Cu^{2+} ions was estimated as 20 μM from both single and dual metal ion titrations. Therefore, the quencher concentration for all metal ions was chosen as 20 μM. Stern–Volmer quenching constants of Cu^{2+} ions clearly reveal the best selective sensitivities of both dendrimers (**TPAD1** and **TPAD2**) with the 1,3,5-triazine-4,6-diamine probe is towards Cu^{2+} ions in comparison with other interfering metal ions, such as Zn^{2+}, Hg^{2+}, Pb^{2+}, Fe^{3+}, and Ag^+. In addition, it was verified that the sensitivity of dendrimer **TPAD2** was relatively higher than that of **TPAD1**. Quenching constant values of **TPAD1** and **TPAD2** towards Cu^{2+} ions were 4.10×10^5 and 1.20×10^6, respectively, and found to be the best reported values in regards to Cu^{2+} ion sensors based on triarylamine dendrimers so far. This new sensory probe was also known to be specific and selective to Cu^{2+} ions even when mixed with some interfering metal ions, and the reversible nature of the sensor probes with high quenching constant (K_{SV}) values were also proven by the addition of pentamethyl ethylene triamine (**PMDTA**). Finally, it was well established that 1,3,5-triazine-4,6-diamine probe with good fluorophores can act as selective and sensitive sensors towards Cu^{2+} ions. Specific selectivities of both dendrimers to Cu^{2+} ions in the presence of 19 interfering metal ions were confirmed by the Stern–Volmer quenching constants (K_{SV}) of all metal ions.
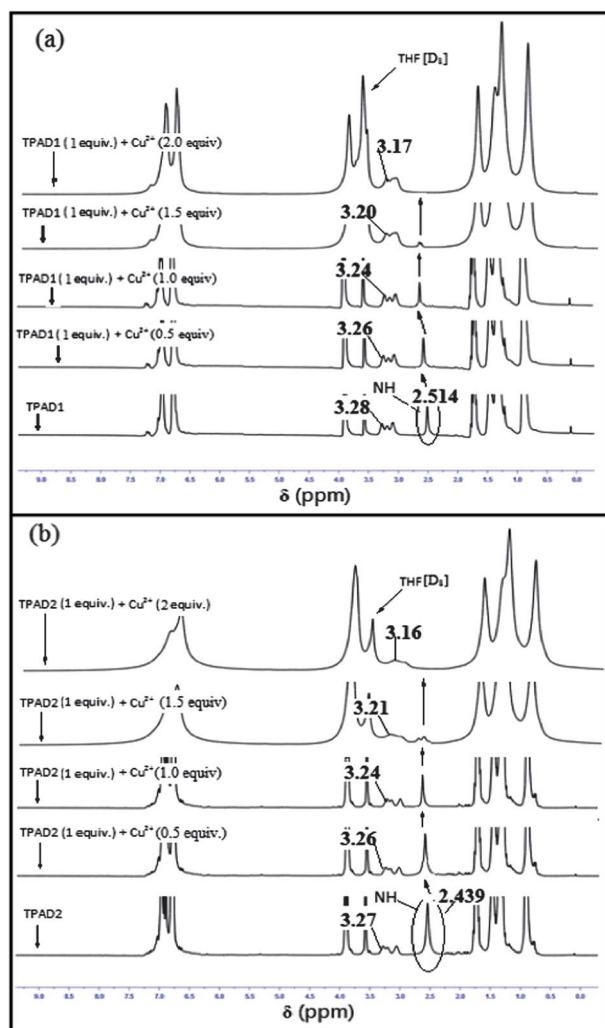
8984 | *J. Mater. Chem.*, 2012, **22**, 8976–8987

This journal is © The Royal Society of Chemistry 2012

Fig. 10 (a) and (b) H^1 NMR spectra of 1 equiv. of **TPAD1** and **TPAD2** (1×10^{-3} M in [D$_8$] THF) with 2 equiv. of Cu^{2+} (2×10^{-2} M in D$_2$O); the final solvent composition after titrations was [D$_8$] THF : D$_2$O = 2 : 1 in vol.
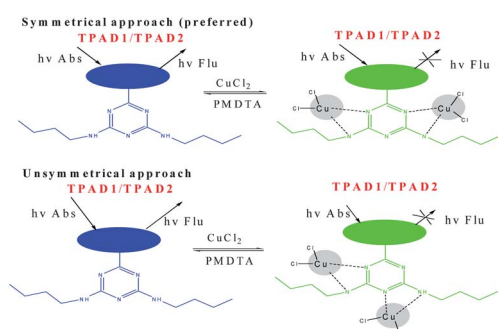

Fig. 11 Possible approach mechanism of Cu^{2+} ions towards the triazine core.

Conclusions

Two novel fluorescent triarylamine-based dendrimers **TPAD1** and **TPAD2** with a new N^4,N^6-dibutyl-1,3,5-triazine-4,6-diamine probe were synthesized *via* normal synthetic routes and for the
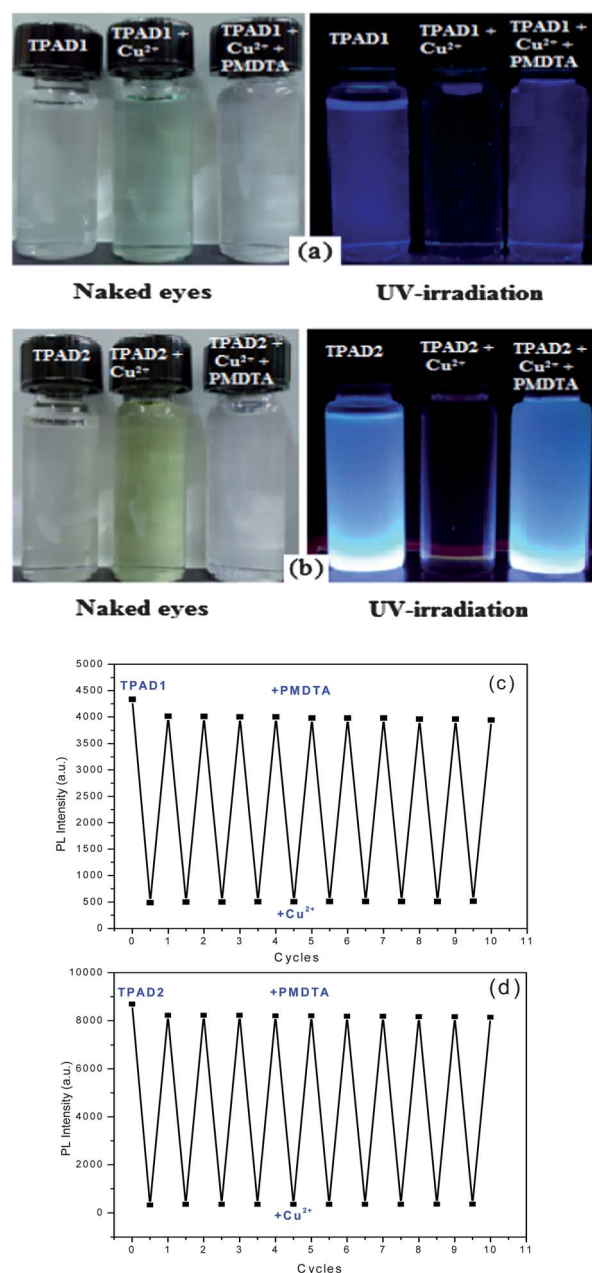

Fig. 12 Reversibility of (a) **TPAD1** and (b) **TPAD2** visualized by the naked eye and UV-light irradiations. (c, d) Reversible sensor cycles of **TPAD1** and **TPAD2**, respectively.

first time they were utilized for dual applications such as electron/energy transfers in H-bonded supramolecules as well as in chemosensors. Both dendrimers (**TPAD1** and **TPAD2**) formed H-bonded donor–acceptor–donor (D–A–D) supramolecular triads (**TPAD1-PBI-TPAD1** and **TPAD2-PBI-TPAD2**) with **PBI**. The presence of multiple H-bonds in solution state was elucidated by ^{1}H NMR titrations and IR spectral studies. J-aggregations and electron/energy transfers provided by both dendrimers were established by UV–Vis and PL titrations with **PBI** and the nanostructural sizes of the supramolecular triads were evaluated by X-ray diffraction (XRD) analysis. In similar manners, both dendrimers also shows their best sensing selectivities towards
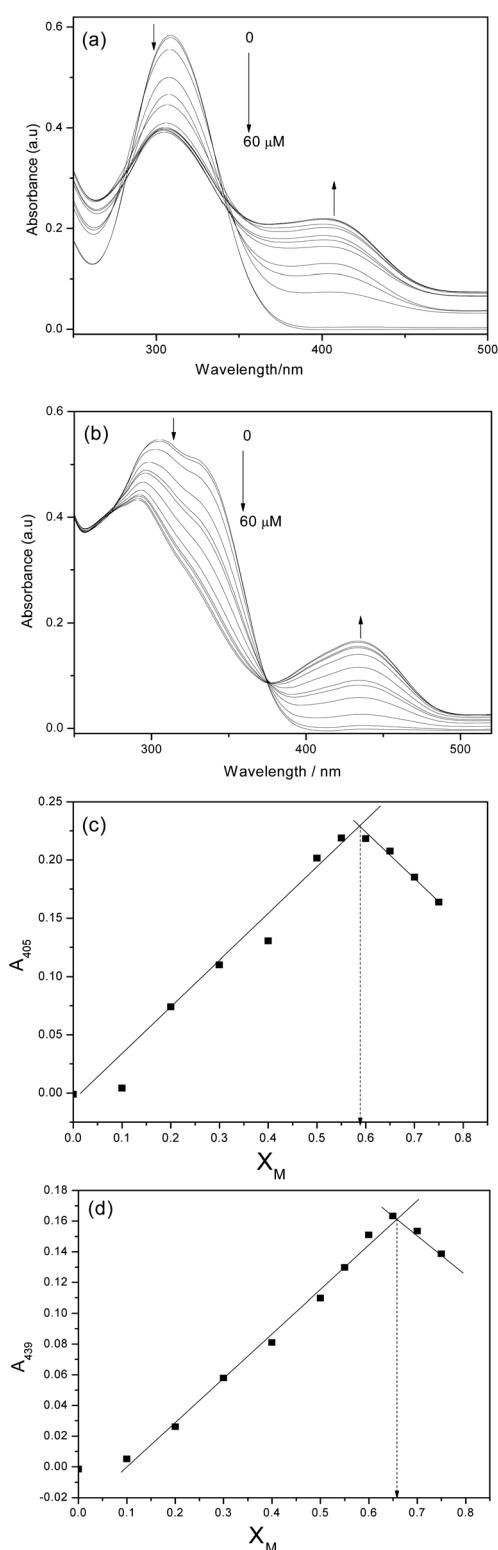
Fig. 13 UV–Vis titrations of (a) **TPAD1** (20 μM in THF : H₂O = 4 : 1 in vol.) and (b) **TPAD2** (20 μM in THF : H₂O = 4 : 1 in vol.) upon addition of Cu²⁺ (0, 2, 6, 10, 14, 20, 26, 30, 32, 38, 46, 52, 58, and 60 μM) solution in H₂O; Job plot for determining the stoichiometry of (c) **TPAD1** and Cu²⁺ ions (THF : H₂O = 2 : 1 in vol.) and (d) **TPAD2** and Cu²⁺ ions (THF : H₂O = 2 : 1 in vol.). The variation of the absorption at 405 nm (**TPAD1**) and 439 nm (**TPAD2**) were measured as a function of molar ratio X_M = [Cu²⁺]/{[Cu²⁺] + [**TPAD1**] or [**TPAD2**]}.

Cu²⁺ ions among the 20 selected metal ions (at 10^{-5} M levels) in semi-aqueous media (THF : H₂O = 2 : 1 in vol.), and **TPAD2** provides a higher sensitivity than **TPAD1**. Therefore, it confirms that the higher generation of a dendritic structure with a larger number of fluorescent units was required for the higher sensitivity towards specific metal ions. In general, both dendrimers have specific selectivities towards Cu²⁺ ions, even in the presence of other interfering metal ions, such as Zn²⁺, Hg²⁺, Pb²⁺, Fe³⁺, and Ag⁺. Moreover, the detection limit of Cu²⁺ ions by these dendrimers were estimated as 20 ppm by fluorescence titrations in THF : H₂O = 2 : 1 in vol., and the binding site deduced as N^4,N^6-dibutyl-1,3,5-triazine-4,6-diamine probe from ¹H, ¹³C NMR titrations in [D₈] THF : D₂O = 2 : 1 in vol. The stoichiometry of Cu²⁺ complexes formed during the sensor process was established as 1 : 2 from the Job plot method based on UV–Vis titrations and the preferred complex formation mechanism was proposed.

Acknowledgements

Notes and references

1 S. C. Lo and P. L. Burn, *Chem. Rev.*, 2007, **107**, 1097–1116.
2 U. D. Astruc, E. Boisselier and C. Ornelas, *Chem. Rev.*, 2010, **110**, 1857.
3 S. H. Ainsa, R. Alcala, J. Barbera, M. Marcos, C. Sanchez and J. L. Serrano, *Macromolecules*, 2010, **43**, 2660.
4 M. A. Mintzer and M. W. Grinstaff, *Chem. Soc. Rev.*, 2011, **40**, 173.
5 F. C. De Schryver, T. Vosch, M. Cotlet, M. V. Auweraer, K. MQllen and J. Hofkens, *Acc. Chem. Res.*, 2005, **38**, 514.
6 L. Brunsveld, B. J. B. Folmer, E. W. Meijer and R. P. Sijbesma, *Chem. Rev.*, 2001, **101**, 4071.
7 R. P. Sijbesma and E. W. Meijer, *Chem. Commun.*, 2003, 5.
8 R. R. Reghu, H. K. Bisoyi, J. V. Grazulevicius, P. Anjukandi, V. Gaidelis and V. Jankauskas, *J. Mater. Chem.*, 2011, **21**, 7811.
9 F. Wurthner, T. E. Kaiser and C. R. Saha-Moller, *Angew. Chem., Int. Ed.*, 2011, **50**, 3376.
10 (a) E. Pazos, O. Vazquez, J. L. Mascarenas and M. E. Vazquez, *Chem. Soc. Rev.*, 2009, **38**, 3348; (b) A. Gemma, P. Josefina and M. Arben, *Chem. Rev.*, 2011, **106**, 3433.
11 M. F. Yardim, T. Budinova, E. Ekinci, N. Petrov, M. Razvigorova and V. Minkova, *Chemosphere*, 2003, **52**, 835.
12 K. Piontek, M. Antorini and T. Choinowski, *J. Biol. Chem.*, 2002, **277**, 37663.
13 R. G. Mohammad, P. Tahereh, H. B. Leila, R. Shohre, Y. Mohammad, R. K. Maryam, M. Abolghasem, A. Hossein and S. Mojtaba, *Anal. Chim. Acta*, 2001, **440**, 81.
14 (a) K. C. Ko, J. S. Wu, H. J. Kim, P. S. Kwon and J. W. Kim, *Chem. Commun.*, 2011, **47**, 3165; (b) S. Sirilaksanapong, M. Sukwattanasinitt and P. Rashatasakhon, *Chem. Commun.*, 2012, **48**, 293.
15 (a) L. Zeng, E. W. Miller, A. Pralle, E. Y. Isacoff and C. J. Chang, *J. Am. Chem. Soc.*, 2006, **128**, 10; (b) D. W. Domaille, E. L. Que and C. J. Chang, *Nat. Chem. Biol.*, 2008, **4**, 168.
16 J. H. Jung, J. H. Lee and S. Shinkai, *Chem. Soc. Rev.*, 2011, **40**, 4464.
17 G. W. Gokel, W. M. Leevy and M. E. Weber, *Chem. Rev.*, 2004, **104**, 2723.
18 (a) M. M. Hossein, M. Ali, R. Razieh and S. Mojtaba, *Sens. Actuators, B*, 2002, **86**, 222; (b) S. Patra and P. Paul, *Dalton Trans.*, 2009, 8683–8695.
19 R. Joseph and C. P. Rao, *Chem. Rev.*, 2011, **111**, 4658.
20 (a) Y. Zhou, J. Won, J. Y. Lee and J. Yoon, *Chem. Commun.*, 2011, **47**, 1997; (b) J. Li, Y. Wu, F. Song, G. Wei, Y. Cheng and C. Zhu, *J. Mater. Chem.*, 2012, **22**, 478.
21 H. N. Kim, Z. Guo, W. Zhu, J. Yoon and H. Tian, *Chem. Soc. Rev.*, 2011, **40**, 79.

22 (a) I. Grabchev, S. Dumas, J. M. Chovelon and A. Nedelcheva, *Tetrahedron*, 2008, **64**, 2113; (b) P. K. Lekha and E. Prasad, *Chem.– Eur. J.*, 2011, **17**, 8609.

23 (a) V. Balzani, P. Ceroni, S. Gestermann, C. Kauffmann, M. Gorka and F. Vogtle, *Chem. Commun.*, 2000, 853; (b) N. Niamnont, W. Siripornnoppakhun, P. Rashatasakhon and M. Sukwattanasinitt, *Org. Lett.*, 2009, **11**, 2768; (c) N. Niamnont, R. Mungkarndee, I. Techakriengkrai, P. Rashatasakhon and M. Sukwattanasinitt, *Biosens. Bioelectron.*, 2010, **26**, 863.

24 D. G. Mullen, M. Fang, A. Desai, J. R. Baker, Jr., B. G. Orr and M. M. Banaszak Holl, *ACS Nano*, 2010, **2**, 657.

25 (a) J. Li and D. Liu, *J. Mater. Chem.*, 2009, **19**, 7584–759; (b) M. Zhu, J. Zou, S. Hu, C. Li, C. Yang, H. Wu, J. Qin and Y. Cao, *J. Mater. Chem.*, 2012, **22**, 361.

26 (a) M. Thelakkat, *Macromol. Mater. Eng.*, 2002, **287**, 442; (b) N. Satoh, T. Nakashima and Y. Kimihisa, *J. Am. Chem. Soc.*, 2005, **127**, 13030.

27 S. Roquet, A. Cravino, P. Leriche, O. Aleveque, P. Frere and J. Roncali, *J. Am. Chem. Soc.*, 2006, **128**, 3459.

28 (a) D. C. Sherrington and K. A. Taskinen, *Chem. Soc. Rev.*, 2001, **30**, 83; (b) Francisco Vera, J. L. Serrano and T. Sierra, *Chem. Soc. Rev.*, 2009, **38**, 781.

29 (a) M. Pawlicki, H. A. Collins, R. G. Denning and H. L. Anderson, *Angew. Chem., Int. Ed.*, 2009, **48**, 3244; (b) C. Huang, M. M. Sartin, N. Siegel, M. Cozzuol, Y. Zhang, J. M. Hales, S. Barlow, J. W. Perry and S. R. Marder, *J. Mater. Chem.*, 2011, **21**, 16119.

30 (a) F. Würthner, C. Thalacker and A. Sautter, *Adv. Mater.*, 1999, **11**, 754; (b) L. E. Sinks, B. Rybtchinski, M. Iimura, B. A. Jones, A. J. Goshe, X. Zuo, D. M. Tiede, X. Li and M. R. Wasielewski, *Chem. Mater.*, 2005, **17**, 6295.

31 Y. Liu, S. Xiao, H. Li, Y. Li, H. Liu, F. Lu, J. Zhuang and D. D. Zhu, *J. Phys. Chem. B*, 2004, **108**, 6256.

32 L. Horner and R. J. Singer, *Tetrahedron Lett.*, 1969, **10**, 1545.

33 P. Wei, X. Bi, Z. Wu and Z. Xu, *Org. Lett.*, 2005, **7**, 3199.

34 (a) S. Yagai, M. Higashi, T. Kinoshita, K. Kishikawa, T. Nakanishi, T. Karatsu and A. Kitamura, *J. Am. Chem. Soc.*, 2007, **129**, 13277; (b) T. E. Kaiser, V. Stepanenko and F. Wurthner, *J. Am. Chem. Soc.*, 2009, **131**, 6719.

35 (a) Y. Liu, J. Zhuang, H. Liu, Y. Li, F. Lu, H. Gan, T. Jiu, N. Wang, X. He and D. Zhu, *ChemPhysChem*, 2004, **5**, 1210; (b) Y. Liu, Y. Li, L. Jiang, H. Gan, H. Liu, Y. Li, J. Zhuang, F. Lu and D. Zhu, *J. Org. Chem.*, 2004, **69**, 9049.

36 A. P. H. J. Schenning, J. V. Herrikhuyzen, P. Jonkheijm, Z. Chen, F. Würthner and E. W. Meijer, *J. Am. Chem. Soc.*, 2002, **124**, 10252.

37 R. Thangavel, R. S. Moirangthem, W. S. Lee, Y. C. Chang, P. K. Wei and J. Kumare, *J. Raman Spectrosc.*, 2010, **41**, 1594.

38 Y. Cheng, L. Zhao, Y. Li and T. Xu, *Chem. Soc. Rev.*, 2011, **40**, 2673.

39 Z. Ma, F. E. Jacobsen and D. P. Giedroc, *Chem. Rev.*, 2009, **109**, 4644.

40 (a) W. Chen, X. Tu and X. Guo, *Chem. Commun.*, 2009, 1736–1738; (b) B. Ding, Y. Si, X. Wang, J. Yu, L. Feng and G. Sun, *J. Mater. Chem.*, 2011, **21**, 13345.

41 K. L. Haas and K. J. Franz, *Chem. Rev.*, 2009, **109**, 4921.

42 M. Kruppa and B. Konig, *Chem. Rev.*, 2006, **106**, 3520.

43 R. Chakrabarty, P. Sarathi Mukherjee and P. J. Stang, *Chem. Rev.*, 2011, **111**, 6810.

44 H. C. Chu, Y. H. Lee, S. J. Hsu, P. J. Yang, A. Yabushita and H. C. Lin, *J. Phys. Chem. B*, 2011, **115**, 8845.

45 Y. Q. Weng, F. Yue, Y. R. Zhong and B. H. Ye, *Inorg. Chem.*, 2007, **46**, 7749.

46 C. Qin, W. Y. Wong and L. Wang, *Macromolecules*, 2011, **44**, 483.